Hindawi
Science and Technology of Nuclear Installations
Volume 2022, Article ID 4531040, 17 pages
https://doi.org/10.1155/2022/4531040

Research Article

Numerical Study of Natural Circulation Flow in Reactor Coolant System during a Severe Accident

Dae Kyung Choi,[1] **Won Man Park**,[1] **Sung Man Son**,[1] **Kukhee Lim**,[2] **Yong Jin Cho**,[2] **and Choengryul Choi**[1]

[1]*Elsoltec Inc., Yongin, Republic of Korea*
[2]*Korea Institute of Nuclear Safety, Daejeon, Republic of Korea*

Correspondence should be addressed to Choengryul Choi; crchoi@elsoltec.com

Received 27 January 2022; Revised 7 July 2022; Accepted 23 July 2022; Published 29 August 2022

Academic Editor: Iztok Tiselj

The rupturing of steam generator tubes leads to serious accidents in nuclear power plants. It causes radioactive materials to leak into the secondary system and release outside the reactor containment region. Therefore, it is important to model a technique to determine whether the natural circulation within a reactor coolant system (RCS) can cause rupture. In this study, a computational fluid dynamics (CFD) analysis methodology was incorporated as a first step to establish an RCS natural circulation evaluation technique to generate RCS natural circulation input parameters for the MELCOR analysis of thermally induced steam generator tube rupture (TI-SGTR) in nuclear power plants. Benchmarking tests were conducted against existing experimental studies; the results demonstrated a difference of 9.4% or less between the experimental and CFD analysis results with respect to the main evaluation factors. Subsequently, a steam generator tube simplification modeling technique was established for application to nuclear power plants, and CFD analysis was conducted to determine its applicability. The CFD analysis results revealed that when numerous tubes are simplified into one equivalent tube, the thermal flow characteristics generated in the RCS could be distorted. The findings of this research are expected to be helpful in understanding the thermal flow characteristics of natural circulation in the RCS. Further, the findings may potentially serve as a foundation for future CFD analysis research related to the natural circulation in the RCS of nuclear power plants.

1. Introduction

Since the Fukushima accident in 2011, nuclear safety has received increased attention. It has been reported that the rupturing of steam generator tubes can lead to severe accidents in nuclear power plants, which cause significant damage to the reactor core [1], along with blackout accidents, loss of coolant accidents, and complete loss of water supply accidents [2].

In a severe accident, the core starts to heat up, and steam with a relatively high temperature and low density is formed in the center of the core, which has a relatively high steam output compared with the surrounding area. The superheated steam in the periphery of the core moves to the upper plenum through the center of the core and transfers heat to the upper plenum structure. A part of the steam flows into the hot leg, which then flows into the steam generator and enters the outlet plenum from the inlet plenum along the steam generator tubes. Furthermore, the reactor coolant pump operation is interrupted when a power loss accident occurs at a nuclear power plant. As a result, a loop seal is formed between the rear end of the steam generator and reactor coolant pump, causing a natural circulation between the reactor and the steam generator. This reactor coolant system (RCS) natural circulation phenomenon causes the temperature to rise while transferring the heat generated in the core to other parts of the RCS. If the natural circulation is continuously maintained, a thermally induced steam generator tube rupture (TI-SGTR) may occur as the temperature of the steam generator tube rises [3, 4]. As a result, the radioactive materials in the primary system could leak into

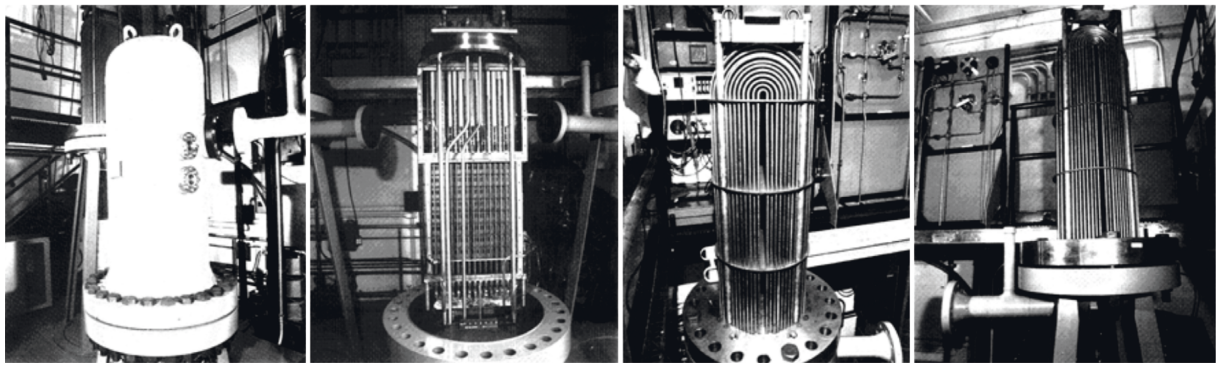

Figure 1: Westinghouse 1/7th scale natural circulation test facility.

the secondary system and get released outside the containment area [5, 6]. Therefore, it is essential to establish natural circulation evaluation techniques that understand the risks of steam generator tube rupture, with research on steam generator tube rupture prevention and management actively ongoing.

Since the steam generator leak incident at the Indian Point Nuclear Power Plant Unit 2 in November 2000, the Nuclear Regulatory Commission (NRC) developed the Steam Generator Action Plan (SGAP) to track and solve the issues associated with steam generators [7, 8]. In May 2001, the SGAP was amended after considering expert opinions about steam generator tubes.

For the experimental research, the Westinghouse Electrical Corporation built an experimental device, scaling down to 1/7th of the Indian Point Unit 2, and installed Westinghouse's Model 44 steam generator to evaluate natural circulation within the RCS [9]. For the numerical research, Idaho National Engineering Laboratory (INEL) identified important variables affecting the formation of the natural circulation flow and analyzed the RCS natural circulation during the damage process and time of occurrence of severe accidents for the Surry power plant using the SCDAP/RELAP5 code [10]. The U.S. NRC used the computational fluid dynamics (CFD) code to analyze the SG-S3 experiment from the Westinghouse 1/7th scale experiments [7]. In addition, comparative verification with Westinghouse's 1/7th scale experimental results and sensitivity analysis for various variables were performed. Subsequently, when the CFD analysis was extended to the full scale [11], a study of the RCS natural circulation was performed for Westinghouse's Model 44 steam generator [8]. The Korea Atomic Research Institute evaluated the SG-S3 experiment from the Westinghouse 1/7th scale experiments and the flow of natural circulation in the OPR1000 RCS using CFD analysis [12]. Nevertheless, there is a lack of research on the RCS natural circulation in nuclear power plants. In addition, when establishing a CFD analysis model for full-scale RCS natural circulation analysis of a nuclear power plant, there is a lack of evaluation of the impact on the generalization ratio of heat transfer tubes.

This study aimed to generate the RCS natural circulation input factors to be used in the MELCOR analysis of TI-SGTR in nuclear power plants. The study is conducted in two stages. The first step is to establish and verify the CFD analysis methodology. The second step is to apply the CFD analysis methodology to a full-scale power plant to derive the natural circulation input factors. Thus, the study serves as the initial step in establishing evaluation methods for natural circulation in the RCS in nuclear reactors. The CFD analysis methodology was validated using existing experimental studies and used to analyze the natural circulation that may arise from pump failure due to the loss of RCS power. Furthermore, a steam generator tube simplification modeling technique was established for use in a nuclear power plant, and its applicability was evaluated.

2. Experimental Validation Analysis

2.1. Validation Experiment. The CFD analysis methodology used in this study was validated in comparison with previous experimental studies [9]. The natural circulation in the RCS was recreated using a 1/7th scale experimental setup designed by Westinghouse and based on the Indian Point Unit 2, wherein a Westinghouse Model 44 steam generator was installed; one reactor and two steam generators were used in this experimental setup.

Figure 1 shows the experimental setup used in this study. The setup included a steam generator installed on either side of the reactor. The reactor and steam generator were connected to the hot leg, which had an inner diameter of Φ 102.3 mm and a total length of 762 mm [9]. The angle of the curved tube connecting the hot leg and inlet plenum was 45°, and its radius of curvature was 160.1 mm. The inner and outer radii of the plenum were Φ 241.3 mm and Φ 254 mm, respectively. The inlet and outlet plenums were separated by a 12.7 mm thick barrier. The tube bundle consisted of a total of 216 pieces, and the tube had an inner and outer diameter of Φ 7.7 mm and Φ 9.5 mm, respectively. The average length of the tube was 2,499.4 mm, the average radius of curvature of the U tube was 101.4 mm, and the total height of the tube bundle was 1,423.9 mm. Each tube was arranged in a triangular array with a pitch of 20.6 mm between the tubes. In this study, CFD analysis was conducted for the Westinghouse SG-S3 experiment.

2.2. CFD Analysis Method. To validate the RCS natural circulation experiment, Ansys Fluent, a commercial CFD code based on the finite volume method, was used. Three main physical phenomena were considered for analyzing the natural circulation in the RCS, namely, the three-

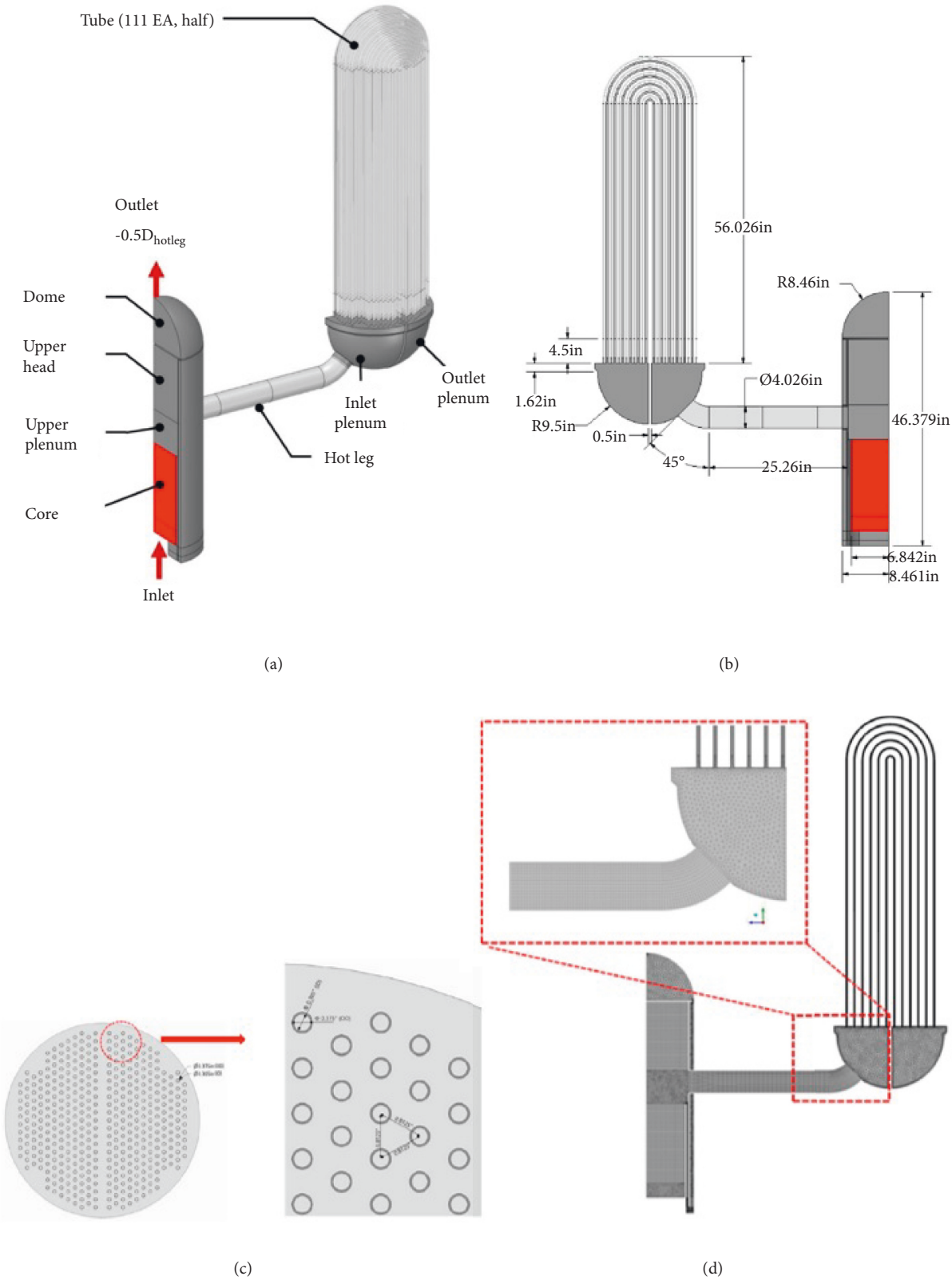

Figure 2: Three-dimensional computer-aided design (CAD) and mesh model in model 1. (a) CAD isometric view, (b) CAD side view, (c) CAD top view, and (d) mesh.

Table 1: Analysis conditions.

Location	Setting (base case)
Working fluid	SF_6
Operating pressure	2,068,427 Pa
Secondary side temperature (tube wall)	337.85 K (64.7°C) (Inlet: 51.4°C, outlet: 66.1°C)
Tube wall	Convective heat transfer (outer surface) $h_{ext} = 250\ W/m^2K$ $T_{ext} = 337.85\ K$
Reactor and hot leg	No-slip wall
Plenum and tube sheet wall	Adiabatic
Reactor-hot leg interface	Porous jump

dimensional compressible flow, turbulent flow, and conjugate heat transfer in the steam generator tube. The continuity equation (equation (1)), momentum equation (equation (2)), and energy equation (equation (3)) were used to simulate each physical phenomenon [13].

$$\frac{\partial \rho}{\partial t} + \nabla(\rho \vec{V}) = 0, \tag{1}$$

$$\frac{\partial}{\partial t}(\rho \vec{V}) + \nabla(\rho \vec{V}\vec{V}) = -\nabla p + \nabla(\tau) + \rho \vec{g} + \vec{F}, \tag{2}$$

$$\frac{\partial}{\partial t}(\rho E) + \nabla(\vec{V}(\rho E + p)) = \nabla\left(k_{eff}\nabla T - \sum h_j \vec{J}_j + \left(\tau_{eff}\vec{V}\right)\right) + S_h. \tag{3}$$

In addition, the standard k–ε model, k–ω shear stress transport (SST) model, and Reynolds stress model (RSM) were considered for the boundary layer properties affected by turbulent flow and process the turbulent viscosity. The k–ε model is the most common turbulence model, and it is suitable for simulating the free-shear layer flow conditions with relatively small pressure gradients. The k–ω SST model has the advantage that it can be used for a relatively wide range of turbulence intensity because the boundary layer approximation equation is selectively used according to flow conditions. The k–ε turbulence model and the k–ω SST model are two-equation turbulence models. The RSM is a turbulence model that can guarantee high accuracy for a flow with a rotational component. However, because it is a six-equation model, it has a disadvantage in that the calculation intensity is relatively higher than the k–ε and k–ω SST models. Previous studies used RSM [7, 8, 11] or k–ω SST turbulence model [12] for RCS natural circulation analysis. The RSM, which was significantly consistent with the experimental results, was selected as the turbulence model in this study.

To model the RCS natural circulation phenomenon, the conditions under which the natural circulation phenomenon occurs were applied. A high-temperature fluid was supplied from the reactor core, and the flow to the cold leg of the outlet plenum was blocked. The inflow rate of the hot leg was maintained the same as the experimental conditions. The fluid region inside the steam generator tube was modeled. Thin wall and outside convective heat transfer conditions were applied to consider the internal/external convective heat transfer and conduction heat transfer of the steam generator tube. Cooling of the working fluid in the steam generator tube is modeled to simulate the RCS natural circulation.

2.3. Geometry and Mesh of the Model. In this study, the scaled-down experimental device used to simulate natural circulation in the RCS was the subject of analysis [9]; the areas from the reactor to the steam generator past the hot leg were considered during model construction for CFD analysis (Figure 2). Previously available experimental research did not specify the reactor dimensions; thus, a commercial nuclear power plant reactor was used to model a virtual reactor, 1/7th of the original scale, with a height of 1.184 m. A porous jump was added to the interface between the reactor and hot leg to rectify the errors caused by uncertainties (because the flow rate of the coolant entering the hot leg from the reactor may vary). Furthermore, models were created for the core, upper plenum, upper head, and dome of the reactor. The simulation was modeled with a complex mesh system using tetrahedral and hexahedral elements, and layered meshes were used in the wall to accurately reproduce heat transfer. The mesh size was determined through a preliminary assessment; a total of 6,360,000 mesh elements were used, with their sizes ranging from 1 to

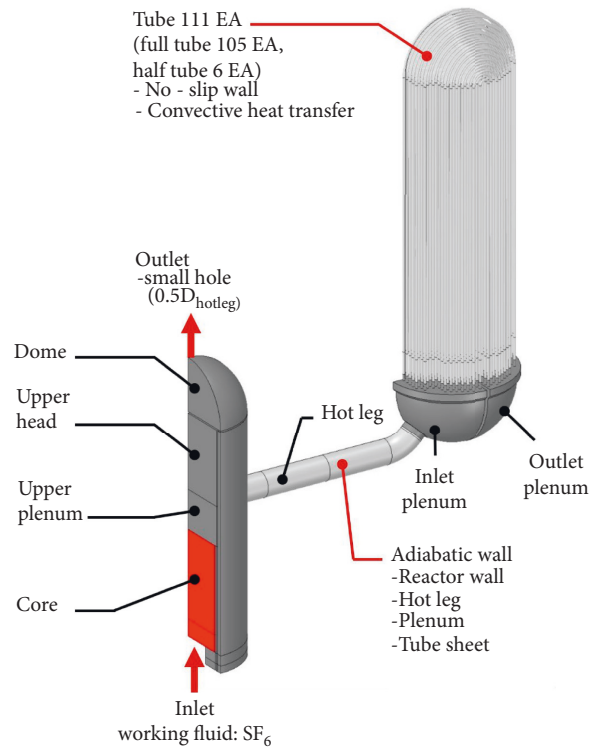

Figure 3: Boundary conditions.

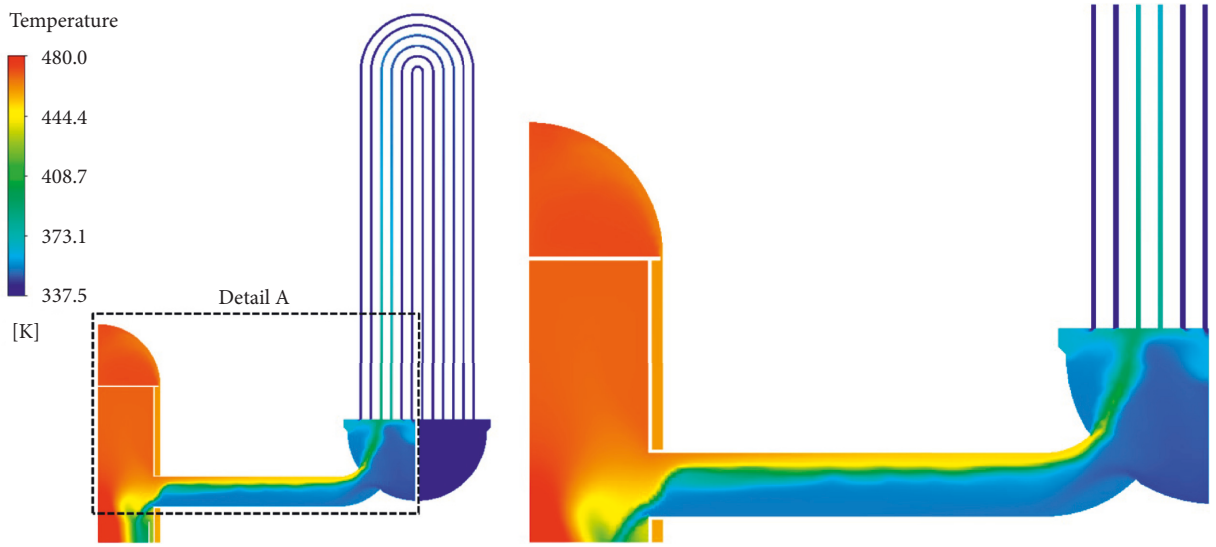

Figure 4: Temperature distribution on symmetry plane (model 1).

10 mm (Figure 2(d)). Approximately 1,659,000 mesh elements were used in the hot leg and nuclear reactor. The mesh size in the hot leg was 0.005 m, and the mesh size in the nuclear reactor was 0.0015~0.01 m. The inlet/outlet plenums used approximately 1,252,000 mesh elements, with mesh sizes ranging from 0.001 to 0.01 m. The number of mesh elements used in the heat pipe was 3,449,000, and sweep meshing was applied. The mesh element size was 0.004 m near the plenum and 0.01 m in the middle region.

2.4. Boundary Conditions of the Model. Analysis conditions for validating the CFD model are presented in Table 1 and Figure 3. SF_6 was used as the working fluid, with an operating pressure of 2,068 kPa (=300 psia). The flow inlet condition was applied to the lower part of the reactor core, and the temperature and flow rate of SF_6 passing the reactor inlet were adjusted to ensure that they correspond to the experimental parameters (447.5 K and 0.23 kg·s^{-1}, respectively). The fluid region inside the tube was modeled, and the

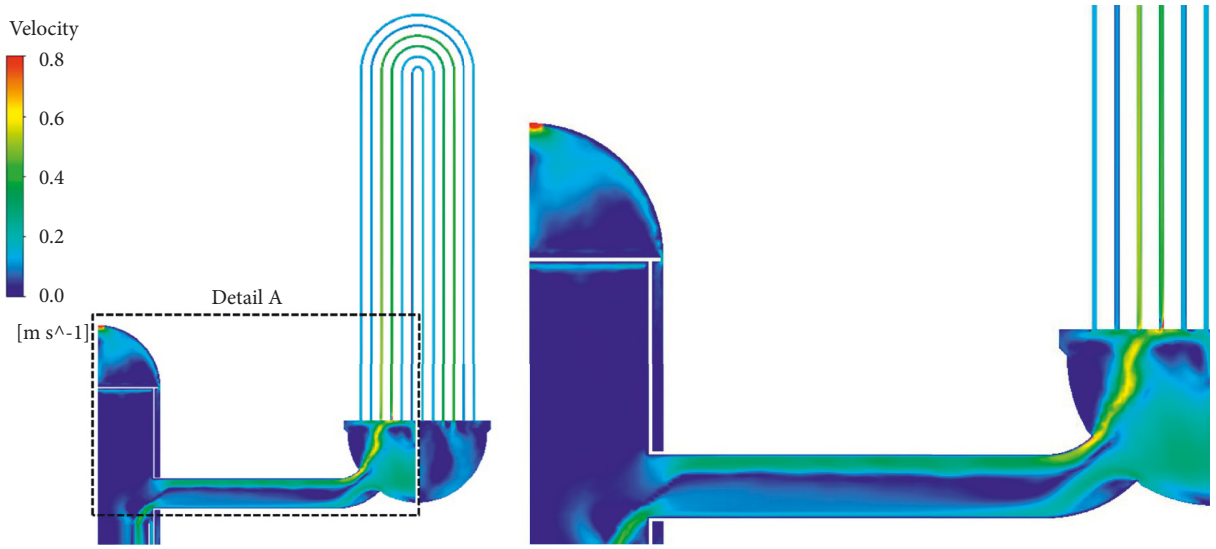

Figure 5: Velocity distribution on symmetry plane (model 1).

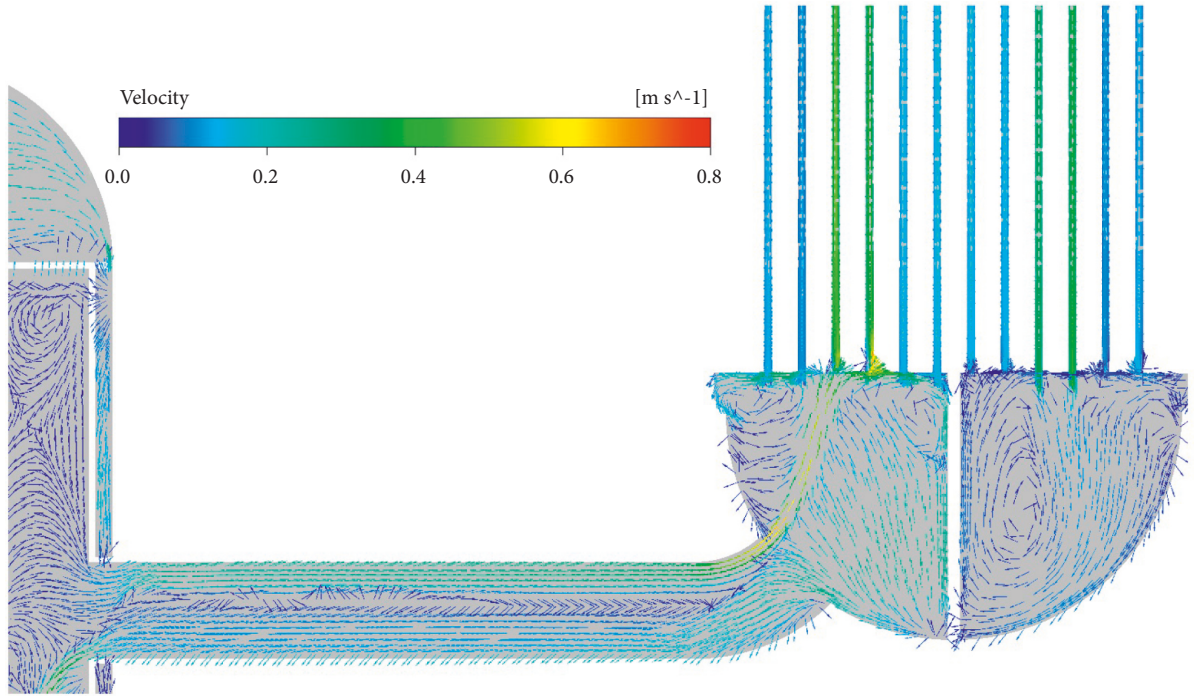

Figure 6: Velocity vector on symmetry plane (model 1).

convective heat transfer conditions at the outer surface of the tube were applied to simulate cooling in the hot fluids through heat exchange as they flowed through the steam generator tube to the secondary system. The convective heat transfer inside the tube was calculated using the energy equation of the RSM model. One-dimensional conduction heat transfer in the tube was calculated using the thermal resistance (R_t), as shown in equation (4). The tube thickness was 0.889 mm, and the thermal conductivity of the tube was 16.2 $Wm^{-1}{\cdot}K^{-1}$ (Table 1). Convection heat transfer outside the tube was calculated using equation (5). The temperature (T_{ext}) of the secondary system (64.7°C/337.85 K) in an existing experiment [9] was used; a convection heat transfer coefficient (h_{ext}) of 250 $Wm^{-2}{\cdot}K^{-1}$ was defined similarly to that in a previous study [7]. The insulation condition was applied to all areas except the tube bundle to prevent heat transfer. In the analysis, the physical properties of SF_6 were treated as a function of temperature, similar to the previous study [7].

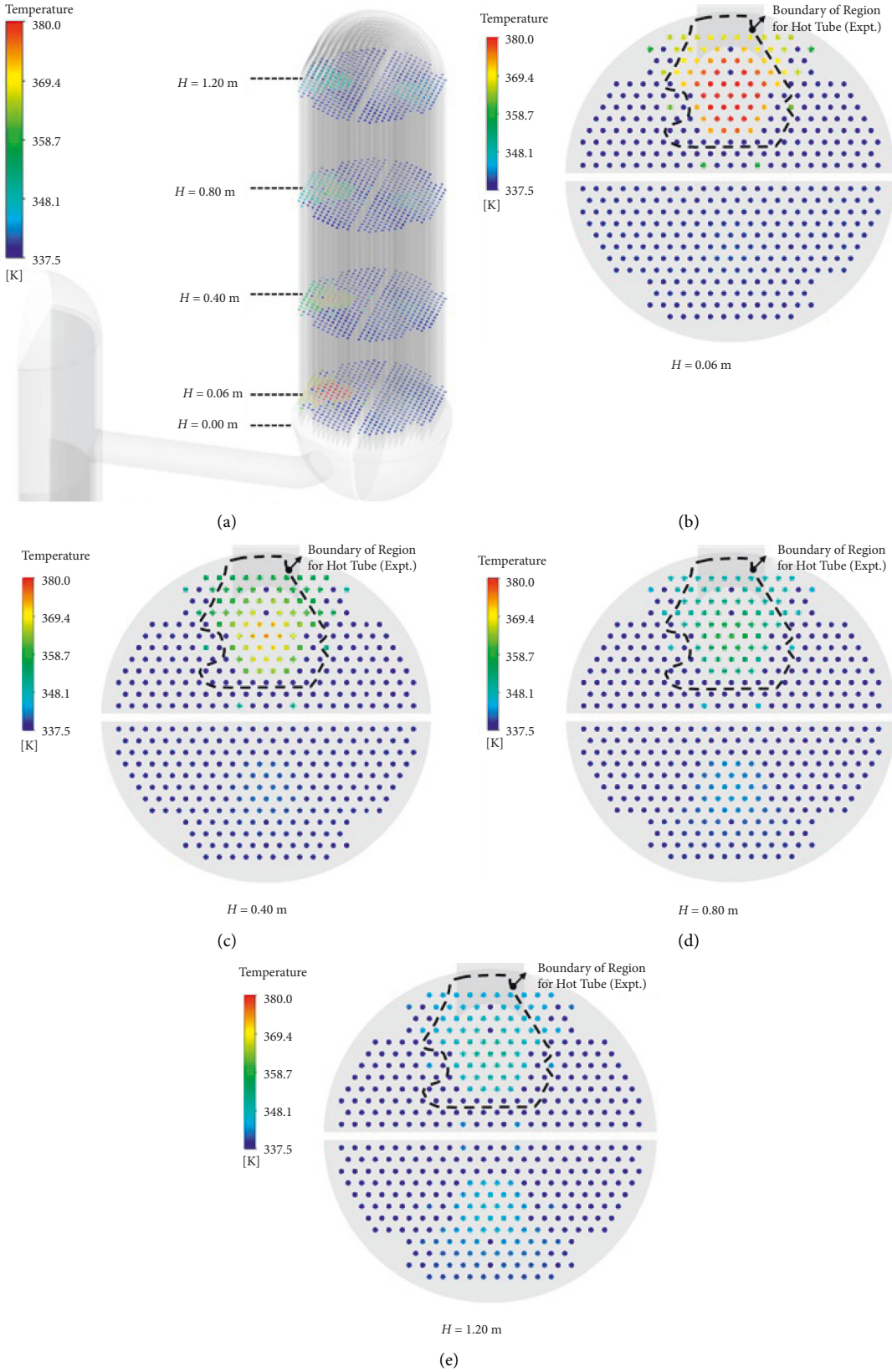

FIGURE 7: Temperature distribution on vertical plane (model 1). (a) Isometric view, (b) H = 0.06 *m*, (c) H = 0.40 *m*, (d) H = 0.80 *m* and (e) H = 1.20 *m*.

Table 2: Comparison of the main evaluation factors between previous studies and CFD analysis.

Contents			Symbol or eq.	EPRI-TR-102818 [9]	NUREG-1781 [7]	Model 1 (present work)
Geometry			—	Reactor-HL-SG	HL-SG	Reactor-HL-SG
Method			—	Experiment	CFD	CFD
End of hot leg	Mass flow rate at the end of hot leg (kg/s)		m_{HL}	0.0599	0.0586 (−2.2%)	0.0610 (1.8%)
	Average temperature (°C)	Hot flow	T_h	159.3	155 (−2.7%)	153.1 (−3.9%)
		Cold flow	T_c	86.8	80.1 (−7.7%)	80.4 (−7.4%)
	Number of hot tubes		—	75	82 (9.3%)	70 (−6.7%)
	Number of cold tubes		—	141	134 (−5.0%)	146 (3.5%)
Tube bundle	Mass flow rate at tubes (kg/s)		m_t	0.1200	0.1206 (0.5%)	0.1199 (-0.1%)
	Heat transfer rate (W)		—	3,560	3,690 (3.7%)	3,591 (0.9%)
	Average temperature (°C)	Hot tube	T_{ht}	100.8	100 (−0.8%)	101.2 (0.4%)
		Cold tube	T_{ct}	64.7	64.7 (0.0%)	64.7 (0.0%)
	Ratio of mass flow rate		m_t/m_{HL}	2.00	2.06 (3.0%)	1.97 (−1.5%)
	Mixed temperature (°C)		T_m	96.2	94.2 (−2.1%)	94.5 (−1.8%)
	Mixing fraction		f	0.85	0.80 (−5.9%)	0.77 (−9.4%)

HL: hot leg; SG: steam generator.

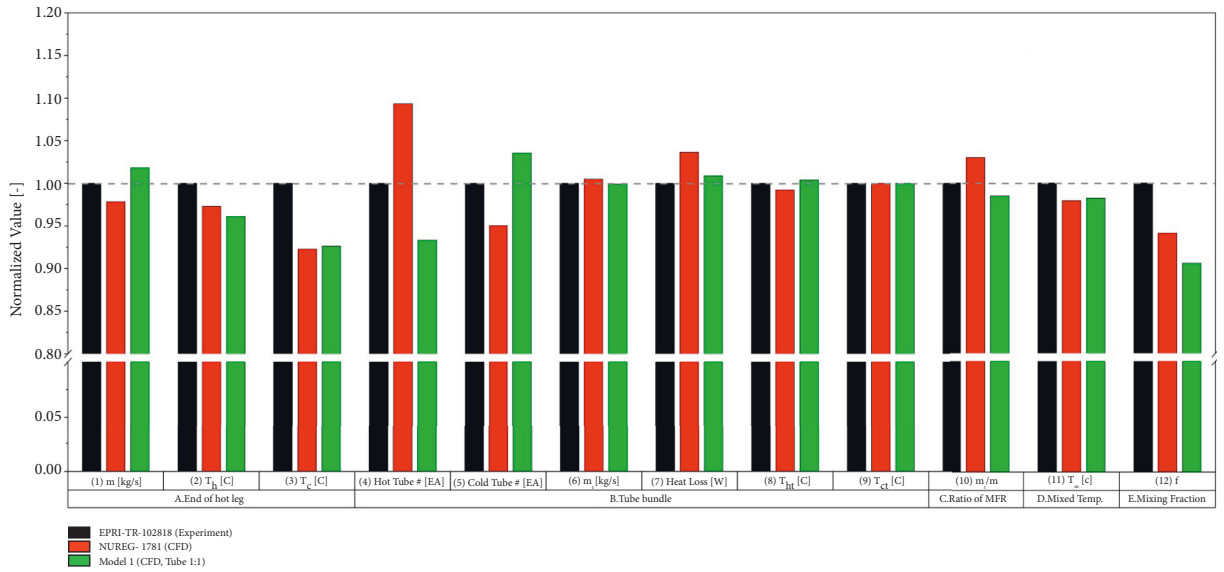

Figure 8: Comparison of the main evaluation factors between previous studies and CFD analysis (normalized value).

$$R_t = \frac{\Delta x}{k}, \tag{4}$$

$$q = h_{\text{ext}}\left(T_{\text{ext}} - T_w\right). \tag{5}$$

2.5. Results and Discussion of the Model. The temperature, velocity contours and velocity vectors on the symmetry plane, and the temperature distribution in the horizontal section of the steam generator tube are shown in Figures 4–6. SF_6 flowing in the reactor core bottom had a high temperature; it flowed through the upper plenum into the upper area of the hot leg and into the steam generator. Despite a single channel, a counterflow was generated in the hot leg. The upper part of the hot leg had a high-temperature distribution, while the lower part had a low-temperature distribution (Figure 4). The flow velocity in the region where high-temperature SF_6 flowed was higher than that in the low-temperature SF_6 region. This phenomenon can be attributed to the narrow cross-section of the flow path in the high-temperature region in comparison with that in the low-temperature region (Figures 5 and 6). The high-temperature SF_6 flowed from the inlet plenum to the outlet plenum, and it was cooled in the steam generator tube. CFD analysis showed that the high-temperature steam generator tube behaved similarly to the experiment (Figure 7). After passing the outlet plenum, the cooled SF_6 entered the steam generator again; then, it entered the hot leg bottom after exiting the steam generator.

On comparing the experimental [9] and CFD analysis results for the main evaluation factors, the differences from the experimental evaluation factors were within −7.7–9.3%

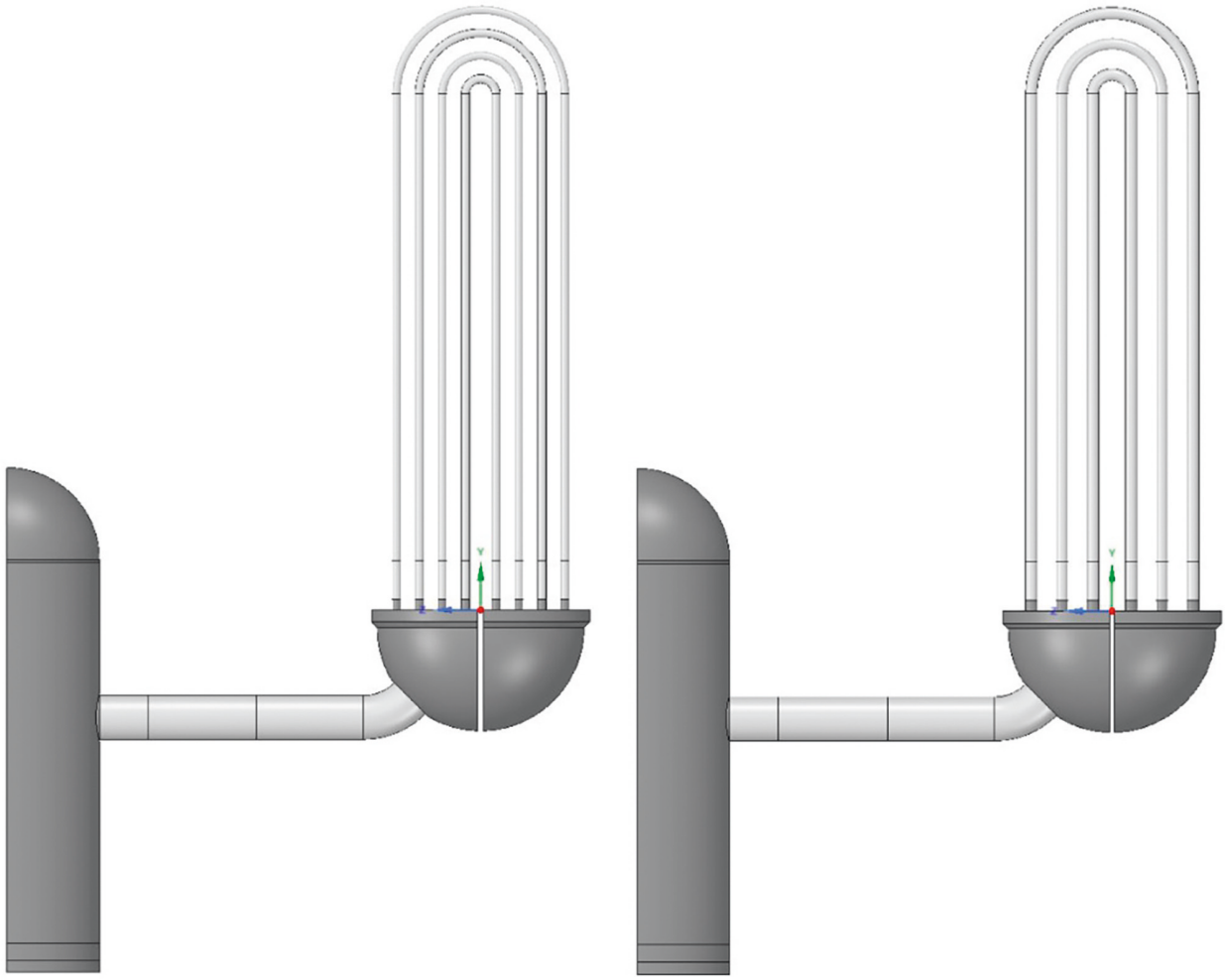

(a) (b)

Figure 9: CAD model of simplified tube in the steam generator. (a) Model 2 and (b) model 3.

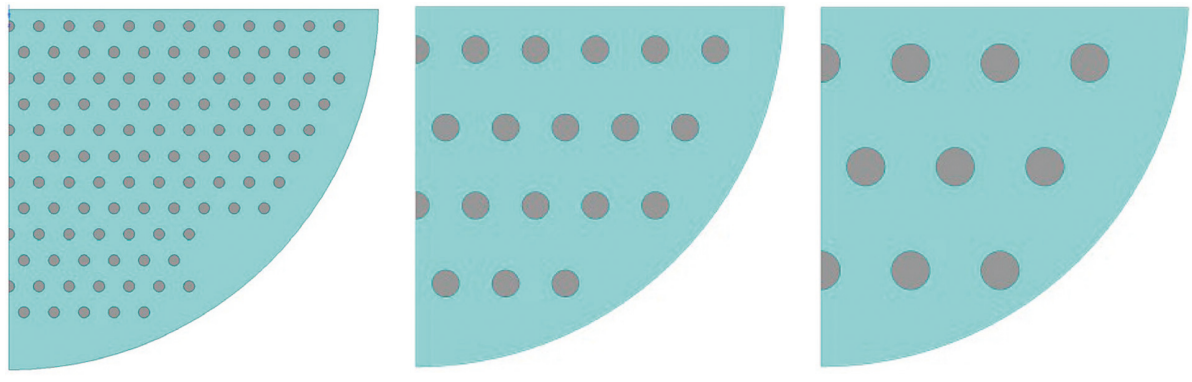

(a) (b) (c)

Figure 10: CAD model of tube arrays. (a) Model 1 (original model). (b) Model 2 (6:1) and (c) model 3 (12:1).

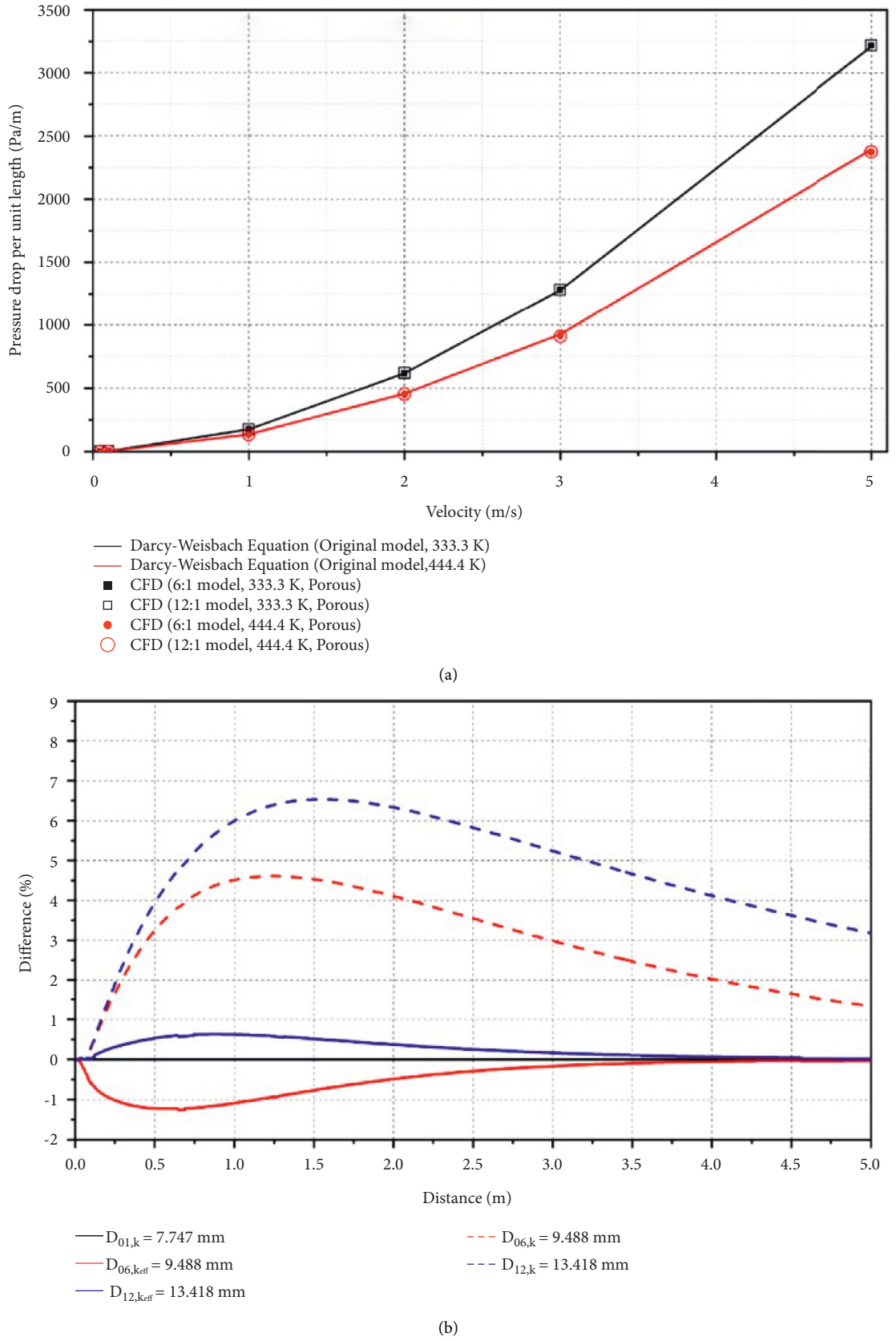

Figure 11: Comparison of pressure drop and temperature properties within steam generator tubes. (a) Pressure drop and (b) temperature difference.

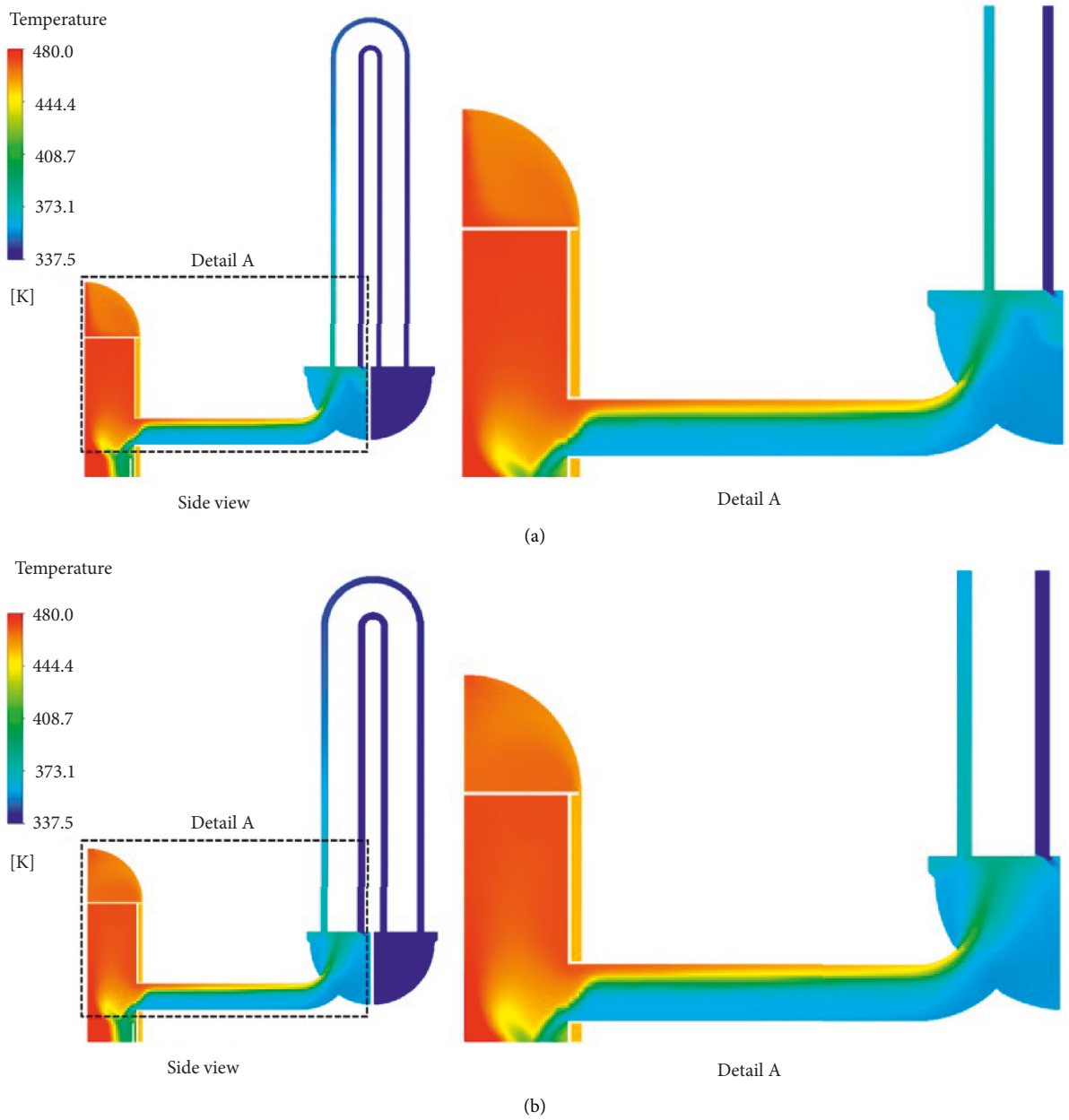

Figure 12: Temperature distribution on symmetry plane (models 2 and 3). (a) Model 2 and (b) model 3.

for the previous study [7] and −3.5–9.4% for this study (Table 2). Thus, it can be concluded that the results of this study are more consistent with existing experimental results than those of previous studies [7, 9].

In the experimental studies performed by Westinghouse and INEEL, water, low-pressure SF_6, and high-pressure SF_6 were used as working fluids. The experimental series using high-pressure SF_6 was suitable for full-scale power plant demonstration simulation. In addition, it was experimentally confirmed that the noncondensable gas does not inhibit the natural circulation phenomenon [10]. Therefore, the RCS natural circulation phenomenon is expected to appear in this analysis model similar to that in the full-scale power plant. However, in the case of a full-scale power plant, the temperature may exceed 1,000 K in a severe accident environment; therefore, the effect of radiation heat transfer should be considered.

3. Analysis of Steam Generator Tube Simplified Model

3.1. Steam Generator Tube Simplification Modeling. CFD analysis requires extensive computational resources for simulating tens of thousands of steam generator tubes to assess the natural circulation in actual nuclear power plants. An analysis method that can reduce the computational resource requirement is desirable. Thus, numerous steam

Table 3: Comparison of the main evaluation factors for each model.

Contents			Symbol or eq.	Experiment	Model 1 Original tube 1 : 1	Model 2 Tube simplification 6 : 1	Model 3 Tube simplification 12 : 1
End of hot leg	Mass flow rate at the end of hot leg (kg/s)		m	0.061 (0.00%)	0.0610 (1.84%)	0.0635 (6.01%)	0.0668 (11.49%)
	Average temperature (°C)	Hot flow	T_h	153.1 (0.00%)	153.1 (−3.89%)	154.3 (−3.14%)	151.0 (−5.24%)
		Cold flow	T_c	86.8 (0.00%)	80.4 (−7.37%)	87.2 (0.46%)	89.0 (2.52%)
Tube bundle	Number of hot tubes		—	75.0 (0.00%)	70.0 (−6.67%)	78.0 (4.00%)	84.0 (12%)
	Number of cold tubes		—	146 (0.00%)	146 (3.55%)	138 (−2.13%)	132 (−6.38%)
	Mass flow rate at tubes (kg/s)		m_t	0.120 (0.00%)	0.120 (0%)	0.126 (4.93%)	0.129 (7.22%)
	Heat transfer rate (W)		—	3,560 (0.00%)	3591 (0.87%)	3,603 (1.2%)	3,473 (−2.44%)
	Average temperature (°C)	Hot tube	T_{ht}	100.8 (0.00%)	101.2 (0.4%)	99.5 (−1.3%)	97.5 (−3.23%)
		Cold tube	T_{ct}	64.7 (0.00%)	64.7 (0%)	64.7 (0%)	64.7 (0.05%)
Ratio of mass flow rate			m_t/m	2.00 (0.00%)	1.97 (−1.5%)	1.98 (−0.85%)	1.93 (−3.67%)
Mixed temperature (°C)			T_m	96.2 (0.00%)	94.5 (−1.77%)	94.7 (−1.52%)	94.2 (−2.08%)
Mixing fraction			f	0.85 (0.00%)	0.77 (−9.41%)	0.84 (−0.97%)	0.89 (4.28%)

generator tubes were modeled in this study as a single tube to reduce the computational intensity. CFD analysis was performed by developing two simplified tube models according to the tube simplification ratio to confirm the applicability to RCS natural circulation analysis.

The simplified tube model increases the cross-sectional area of the flow path compared with the original steam generator tube. Therefore, even if the fluid is cooled through heat exchange with the secondary side, the fluid temperature at the center of the tube can be overestimated, and the pressure loss occurring in the tube can be underestimated. In this case, a flow rate different from the actual flow rate may result from the change in the fluid density or pressure gradient. Therefore, the pressure loss in the steam generator tube was simulated considering the tube interior as a porous media, and an effective fluid thermal conductivity was used in the steam generator tube to accurately model the thermal characteristics.

In model 2, six tubes were modeled as a single equivalent tube, whereas in model 3, 12 tubes were modeled as a single equivalent tube (Figure 9). Each equivalent tube was assumed to be located in the center of the merging steam generator tubes, and the cross-section of the flow path of the steam generator tube before and after simplification was equal (Figure 10).

A comparison of the CFD results for the main evaluation factors with those of previous studies is presented in Table 2 and Figure 8. The flow rate (m_{HL}) of the high-temperature SF_6 flowing from the rear end of the hot leg toward the inlet plenum was 0,0610 kg·s^{-1}, which represented a difference of approximately 1.8% from that in the previous experiment. The average temperature (T_h) of the high-temperature flow at the hot leg rear end was 153.1°C, while the average temperature (T_c) of the low-temperature flow was 80.4°C. The high-temperature SF_6 obtained from the inlet plenum was cooled by passing it through the steam generator tube; its temperature tended to decrease to the level of the secondary system. A total of 70 and 146 high- and low-temperature tubes, respectively, were evaluated in this study. The flow rate (m_t) at the steam generator tube was 0.119 kg·s^{-1}. The average temperature (T_{ht}) of the high-temperature flow into the steam generator tube from the inlet plenum side was 101.2°C; the average temperature (T_{ct}) of the low-temperature flow into the inlet plenum from the steam generator tube was 64.7°C. The ratio (r) between the flow rate (m_t) of the high-temperature flow entering the inlet plenum from the hot leg and the circulation flow rate (m_{HL}) at the steam generator tube was 1.97. The mixed temperature (T_m) of the high-temperature flow entering the inlet plenum from the hot leg and the low-temperature flow entering the inlet plenum from the steam generator tube was 94.5°C. The experimental and CFD results differed by approximately 1.5% and 1.8% for the flow ratio and mixed temperature, respectively. The mixing fraction (f) was a function of the temperature and flow rate of the high-temperature flow from the inlet plenum into the steam generator tube and those of

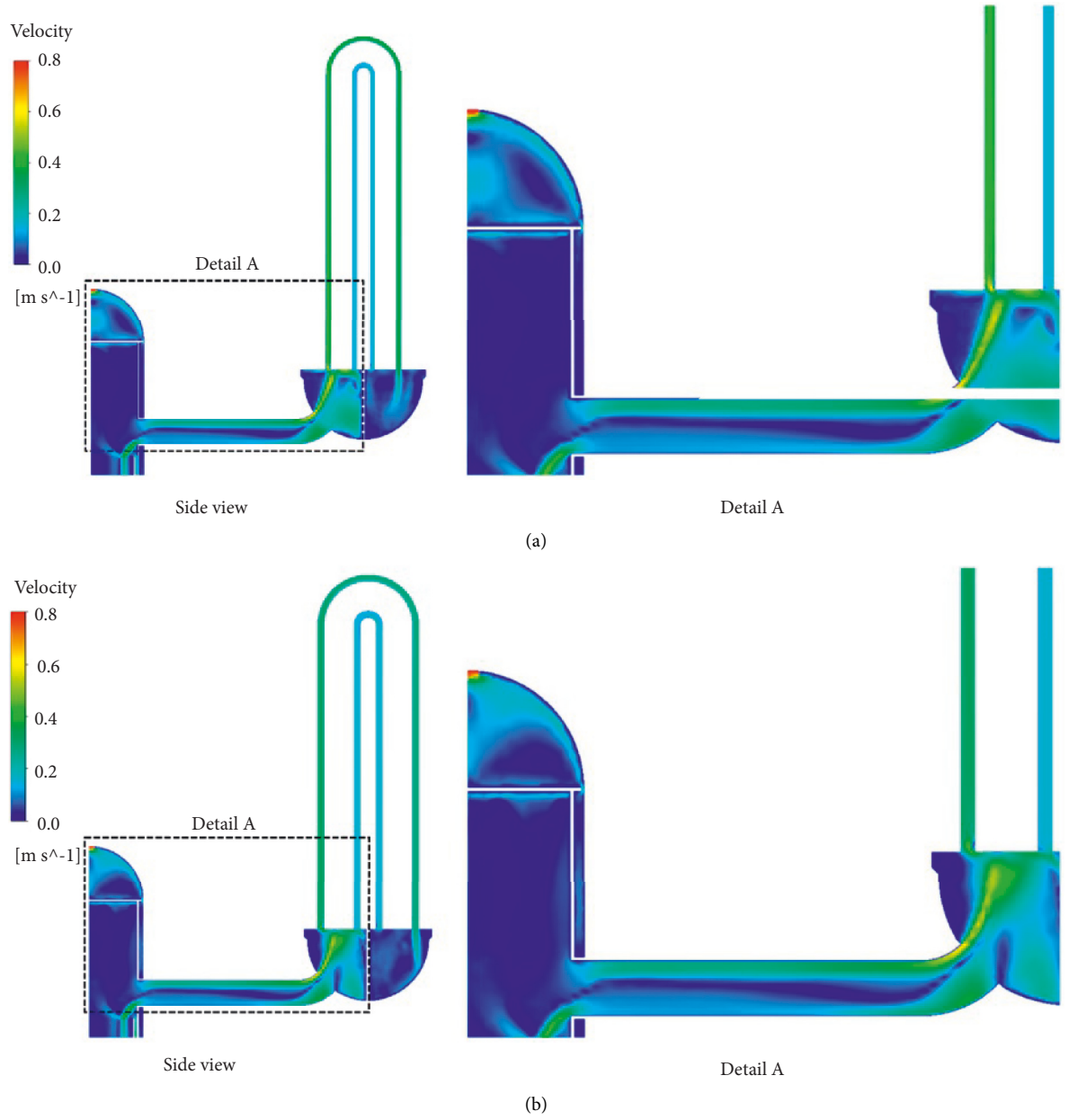

Figure 13: Velocity distribution on symmetry plane (models 2 and 3). (a) Model 2 and (b) model 3.

the high-temperature flow from the hot leg into the inlet plenum. The mixing fraction assessed in this study was 0.77, which differed by 9.4% from the existing experiments. In this study, the mixing temperature (T_m) and mixing fraction (f) were calculated using the following equations:

$$T_m = \frac{1}{1+r}\left(T_h + rT_{\mathrm{ct}}\right), \tag{6}$$

$$f = 1 - r \times \left(\frac{T_{\mathrm{ht}} - T_m}{T_h - T_m}\right). \tag{7}$$

The simplified tube region was modeled as a porous medium to mimic the pressure drop generated in the tube, accurately simulating the pressure drop generated in the original tube. In the previous study, the viscous or inertial resistance coefficient applied to the porous media was fixed; however, in this study, the user-defined function provided by Ansys Fluent was used to model an adjustable inertia resistance coefficient to ensure the generation of pressure drop corresponding to the Reynolds number entering each heat transfer tube [14]. Regarding the conditions for the maximum and minimum temperature of the material properties of SF_6 provided in the previous study [7], the pressure drop per unit length generated at the steam generator tubes (model 1) and the simplified models (models 2 and 3) were evaluated to be comparable (Figure 11(a)).

Compared with the original tubes, the simplified equivalent tubes had a larger inner diameter; consequently, the temperature at the center of the fluid was higher when cooled

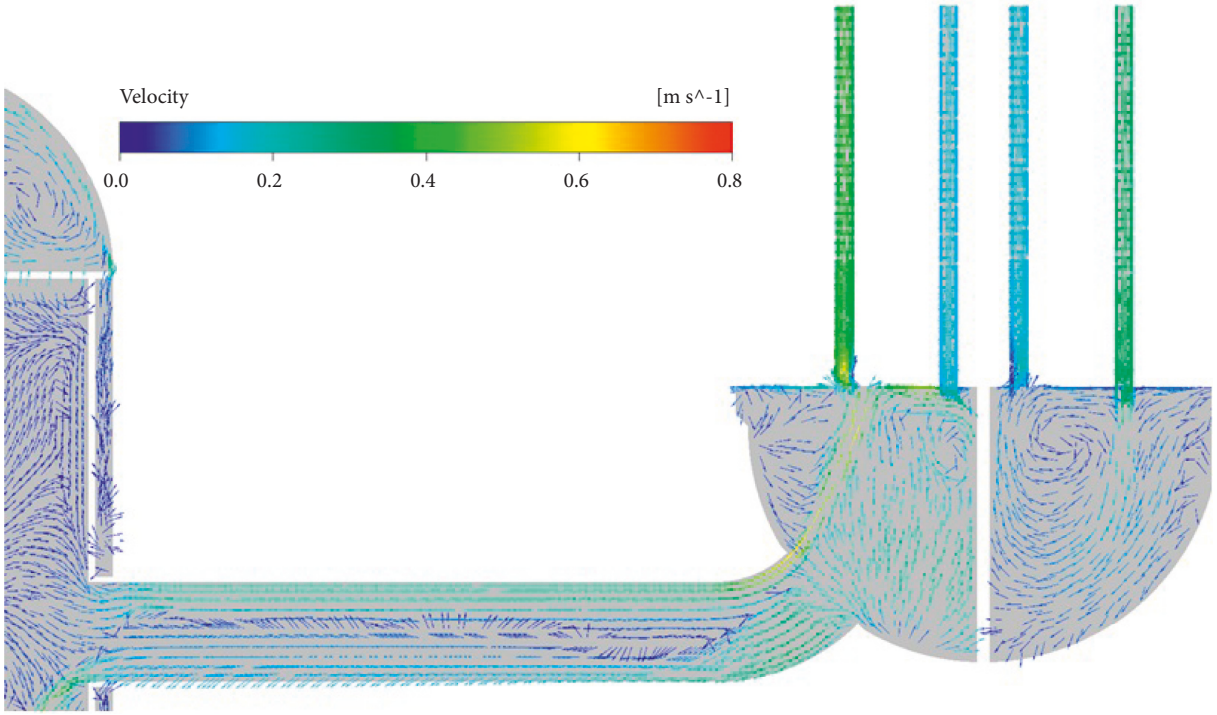

(a)

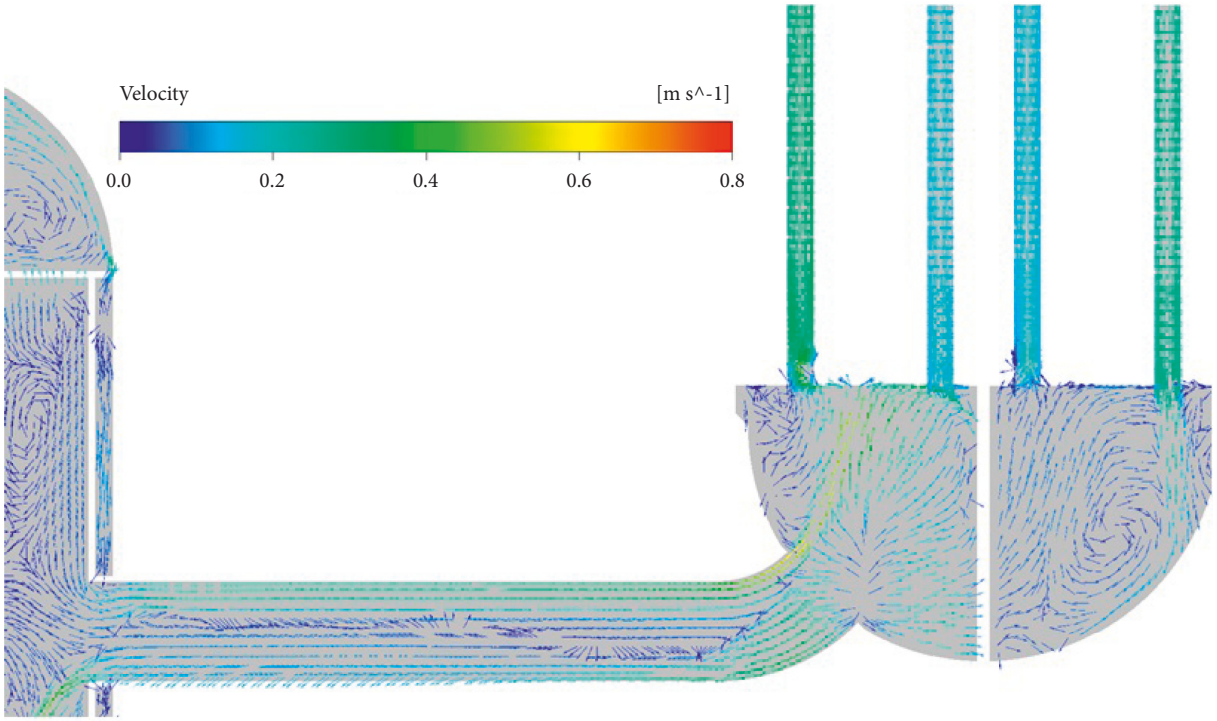

(b)

Figure 14: Velocity vector on symmetry plane (models 2 and 3). (a) Model 2 and (b) model 3.

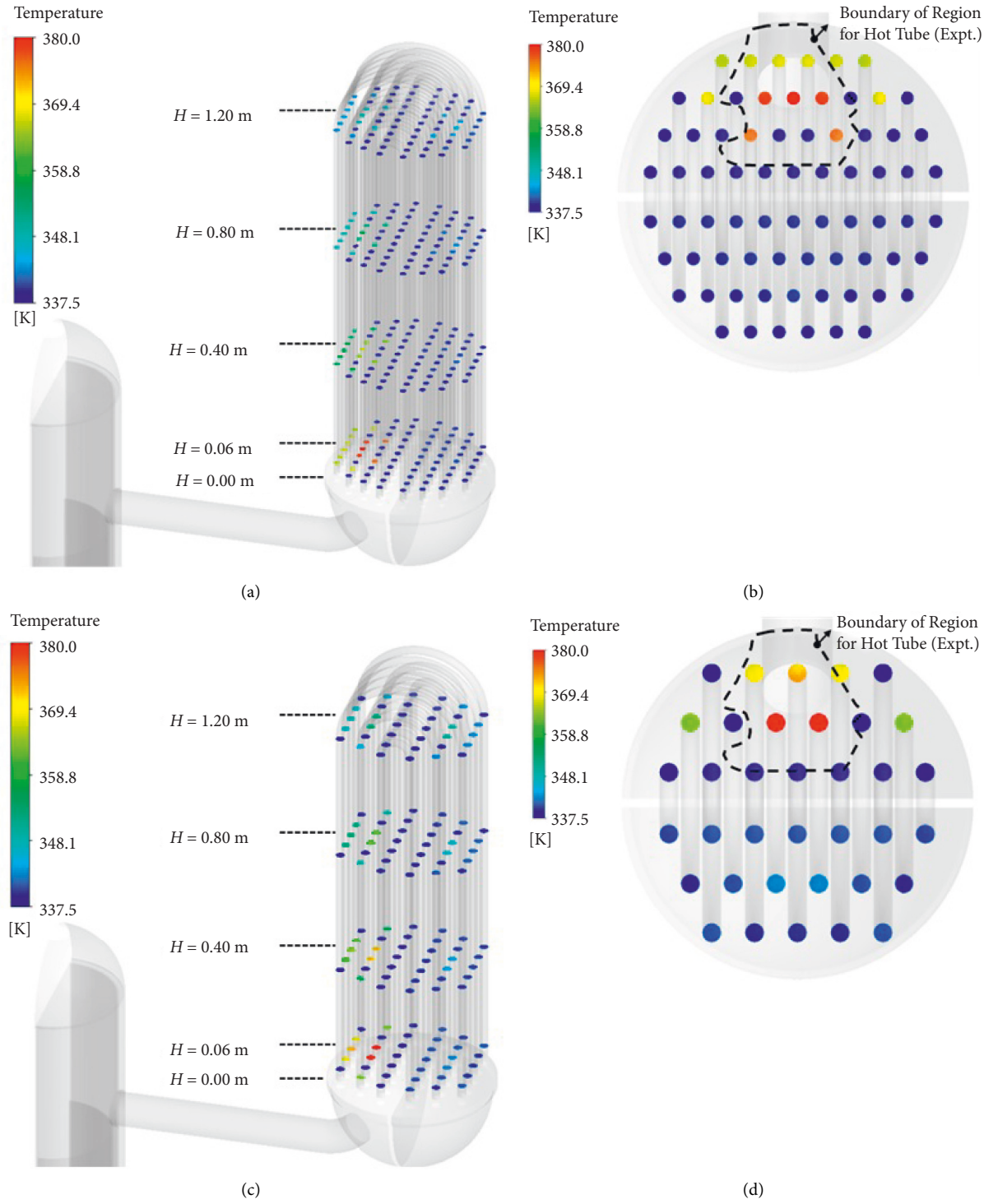

FIGURE 15: Temperature distribution on the vertical plane (models 2 and 3). (a) Model 2 (isometric view), (b) model 2 ($H = 0.06$ m), (c) model 3 (isometric view), and (d) model 3 ($H = 0.06$ m).

with the same heat loss rate. To solve this issue, the effective thermal conductivity (k_{eff}) of the working fluid in the steam generator tube was calculated and applied as follows:

$$k_{\text{eff}} = \varnothing \times k_f + (1 - \varnothing) \times k_s. \quad (8)$$

In this equation, k_f represents the thermal conductivity of the fluid, k_s represents the thermal conductivity of the solid, and $\varnothing$ denotes the porosity. Based on the actual geometry ($ID_{\text{tube}} = 7.747$ mm, $OD_{\text{tube}} = 9.525$ mm) and material of the steam generator tube, $\varnothing = 0.6615$ and $k_s = 16.2$ $\text{Wm}^{-1}\cdot\text{K}^{-1}$ were applied. In this study, SF_6 was used as the working fluid, and its properties were treated as a function of temperature; $k_{eff,\ SF6}$ is in the range of 5.49~5.50 $\text{Wm}^{-1}\cdot\text{K}^{-1}$ depending on the fluid temperature in the heat transfer tube.

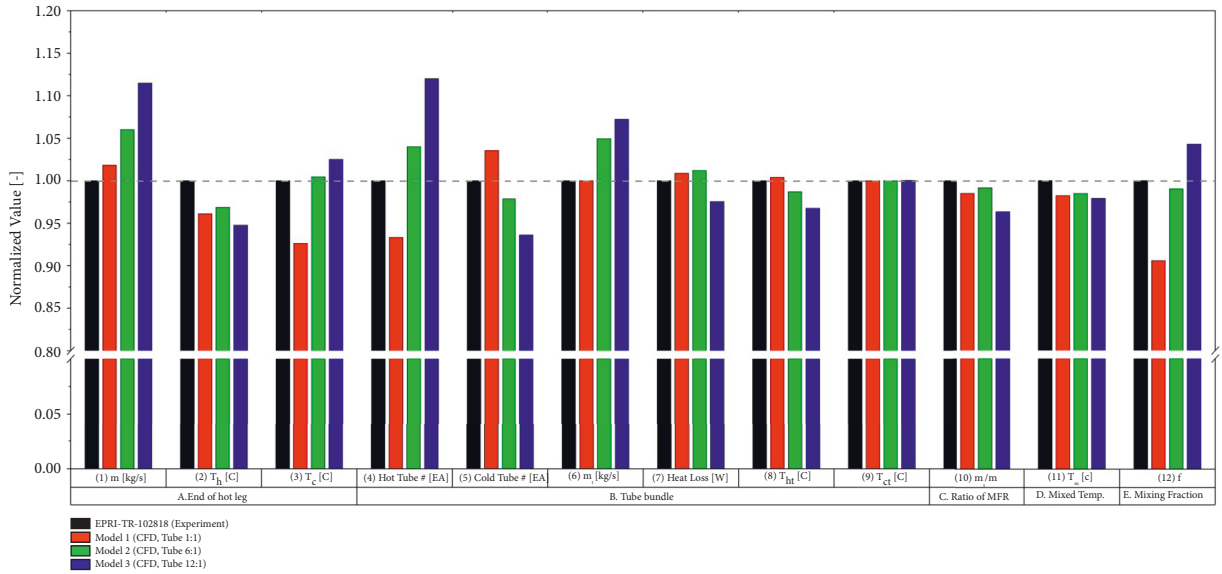

FIGURE 16: Comparison of the main evaluation factors for each model (normalized value).

In full-scale nuclear power plants, the working fluid is steam at a temperature of 1,000 K or higher. The thermal conductivity of steam is ~0.11 $Wm^{-1}\cdot K^{-1}$ at these temperatures, significantly larger than that of SF_6. However, as k_f is significantly smaller than k_s, the effective thermal conductivity of high-temperature steam is expected to be similar to that of SF_6 ($k_{\text{eff, steam, 1000 K}} = 5.55\ W\cdot m^{-1}\cdot K^{-1}$).

To evaluate the validity of the effective thermal conductivity application method, a preliminary CFD analysis was conducted using a straight tube. The steam generator tube was found to be sufficiently longer than the average of 1.382 m when a 5 m straight tube was used. For the straight tube, the inlet temperature was set to 100.8°C (373.23 K) based on the average temperature of the hot tube. An average flow rate was applied in the steam generator tube based on the results of the 1/7th scale experiment. Flow rates of 0.0016, 0.0096, and 0.0192 $kg\cdot s^{-1}$ were applied in models 1, 2, and 3, respectively. The convective heat transfer coefficient at the surface of the straight tube was 250 $Wm^{-2}\cdot K^{-1}$; the external temperature was set to 337.85 K, and the tube thickness was 0.889 mm, similar to the experiment. The fluid temperature at the center of the straight tube was the same as shown in Figure 11(b). The actual tube model and the simplified tube model differed by 4.6–6.5% in terms of temperature when using the fluid thermal conductivity, but the difference decreased to −1.3–0.6% when the effective thermal conductivity was used.

3.2. Geometry and Boundary Condition of Simplified Models. Two simplified steam generator tube models were created with different simplification ratios (models 2 and 3) to evaluate the applicability of RCS natural circulation analysis. The 1/7th scale steam generator contained 216 steam generator tubes, and models 2 and 3 contained 36 and 18 equivalent steam generator tubes, respectively. Because the structure was symmetrical, only one-half of the geometry was analyzed (Figure 9). The other geometries of the inlet and outlet plenums, hot leg, and reactor were identical to those of model 1.

The simplified steam generator tube model was mesh constructed using the same rules as those in the previous experimental validation analysis (model 1). A total of 2,805,000 and 2,566,000 meshes were used in models 2 and 3, respectively.

In this study, the same conditions as those in the SG-S3 experimental validation analysis were applied to the simplified steam generator tube model. The tendencies of the main factors may vary depending on the simplification ratio of the heat transfer tubes; thus, two models (models 2 and 3) were analyzed.

3.3. Results and Discussion of the Simplified Model. The temperature, velocity contours and velocity vectors on the symmetry plane, and the temperature distribution in the horizontal section of the steam generator tube are shown in Figures 12–15. The flow pattern of SF_6 in the steam generator flowing through the upper plenum of the reactor was similar to that of model 1. Table 3 and Figure 16 present a comparison between models 1–3 with previous studies for the main evaluation factors. The results of the experimental tests and CFD analysis differed by 3.1–6.0% and −6.4–12.0% for models 2 and 3, respectively. The results of model 2 were similar to those of model 1, which modeled all steam generator tubes. The steam generator tube could not be cooled to the desired level in model 3 because too many tubes were reduced to one equivalent tube, thereby minimizing the heat transfer surface area of the tube. Based on these results, it can be concluded that the natural circulation can be represented without modeling all tubes if the simplification ratio of the steam generator tubes is appropriately selected for the CFD analysis.

In this study, 216 steam generator tubes were used in the 1/7th scale steam generator model, and two simplified steam generator tube models were considered with a simplification ratio of 6 : 1 and 12 : 1. Sensitivity analysis must be conducted for various simplification ratios to establish the validity of the simplified model of the steam generator tubes because there are numerous tubes in the steam generator of the nuclear power plant.

4. Conclusions

A CFD analysis methodology was established in this study as a first step toward evaluating the natural circulation in the RCS in nuclear power plants. The natural circulation in the RCS caused by pump failure owing to lack of power in the reactor cooling system was evaluated, and benchmarking tests were conducted against existing experimental data. Based on the benchmarking test results, the difference between the experimental and CFD validation analysis results was less than 9.4% (maximally), indicating that the CFD analysis produced similar results as the experiments. For a nuclear power plant, a simplified modeling technique was established for steam generator tubes, and a simplification ratio of 6 : 1 (model (2)) and 12 : 1 (model (3)) was implemented. Further, CFD analysis was conducted to assess the applicability of the simplified modeling technique. The results showed that the thermal flow characteristics of the steam generator could be compromised if an excessive number of heat transfer tubes were simplified into a single equivalent steam generator tube. Consequently, to model simplified steam generator tubes of full-scale power plants in subsequent studies, sensitivity analysis should be conducted for the simplified steam generator tube ratio. In addition to investigating the characteristics of natural circulation in the RCS, the results of this study can be used to validate CFD analysis methods and determine the simplification ratio of steam generator tubes when analyzing RCS natural circulation for full-scale power plants in the future.

Data Availability

Not applicable.

Conflicts of Interest

The authors declare no potential conflicts of interest.

Acknowledgments

This work was supported by the Nuclear Safety Research Program through the Korea Foundation of Nuclear Safety, using financial resources from the Nuclear Safety and Security Commission, Republic of Korea (no. 1805001).

References

[1] *Nuclear Safety Act*, Article 2, Korea Ministry of Government Legislation, Daejeon, South Korea, 2022.

[2] R. J. Park, K. H. Kang, K. S. Ha et al., *Detailed Analysis of a Severe Accident Progression for an Evaluation of In-Vessel Corium Retention Estimation in KSNP (Report No. KAERI/TR-2959)*, Korea Atomic Energy Research Institute, Daejeon, South Korea, 2005.

[3] S. Sancaktar, M. Salay, R. Iyengar, A. Azarm, and S. Majumdar, "Consequential SGTR analysis for Westinghouse and combustion engineering plants with thermally treated alloy 600 and 690 steam generator," Technical report, U.S.NRC, Washington, DC, USA, 2018.

[4] B. C. Lee, S. J. Hong, J. Y. Lee, K. J. Lee, and K. H. Lee, "Development of probability evaluation methodology for high pressure/temperature gas induced RCS boundary failure and SG creep rupture," FNC Technology Co, Yongin, South Korea, 2008.

[5] S. Il Kim, H. Seok Kang, Y. Su Na et al., "Analysis of steam generator tube rupture accident for OPR 1000 nuclear power plant," *Nuclear Engineering and Design*, vol. 382, Article ID 111403, 2021.

[6] Y. Bang, G. Jung, B. Lee, and K. I. Ahn, "Estimation of temperature-induced reactor coolant system and steam generator tube creep rupture probability under high-pressure severe accident conditions," *Journal of Nuclear Science and Technology*, vol. 49, no. 8, pp. 857–866, 2012.

[7] C. F. Boyd and K. Hardesty, "CFD analysis of 1/7th scale steam generator inlet plenum mixing during a PWR severe accident," Technical report, U.S.NRC, Washington, DC, USA, 2003.

[8] C. F. Boyd and K. W. Armstrong, "Computational fluid dynamics analysis of natural circulation flows in a pressurized-water reactor loop under severe accident conditions," Technical report, U.S.NRC, Washington, DC, USA, 2010.

[9] W. A. Stewart, A. T. Pieczynski, and V. Srinivas, *Natural Circulation Experiments for PWR High-Pressure Accidents*, EPRI, Washington, DC, USA, 1993.

[10] P. D. Bayless, D. A. Brownson, C. A. Dobbe et al., *Severe Accident Natural Circulation Studies at the INEL*, Nuclear Regulatory Commission, Washington, DC, USA, 1995.

[11] C. F. Boyd, D. M. Helton, and K. W. Armstrong, "CFD analysis of full-scale steam generator inlet plenum mixing during a PWR severe accident," Technical report, U.S.NRC, Washington, DC, USA, 2004.

[12] H. S. Kang, S. I. Kim, and K. S. Ha, "CFD analysis for producing input parameters of natural circulation flow of a MELCOR analysis for a TI-SGTR accident in the OPR1000," *Journal of Computational Fluids Engineering*, vol. 26, no. 3, pp. 1–10, 2021.

[13] *ANSYS Fluent, ANSYS Fluent Theory Guide, Release 15.0 Documentation, ANSYS Inc., Canonsburg*, Canonsburg, PA, USA, 2017.

[14] I. E. Idelchik, *Handbook of Hydraulic Resistance*, p. 133, Begell House, New York, NY, USA, 2008.